J. Pestic. Sci. **45**(3), 125–131 (2020)
DOI: 10.1584/jpestics.D20-23

Original Article

Biochemical characterization of NADH:FMN oxidoreductase HcbA3 from *Nocardioides* sp. PD653 in catalyzing aerobic HCB dechlorination

Koji Ito,[1] Kazuhiro Takagi,[1,*] Ryota Kataoka[2] and Hiromasa Kiyota[3]

[1] *Hazardous Chemical Division, Institute for Agro-Environmental Sciences, National Agriculture and Food Research Organisation, Kannondai, Tsukuba-city, Ibaraki, Japan*
[2] *Department of Environmental Sciences, University of Yamanashi, Kofu-city, Yamanashi, Japan*
[3] *Graduate School of Environmental and Life Science, Okayama University, Tsushima, Okayama-city, Okayama, Japan*

(Received April 7, 2020; Accepted May 23, 2020)

Nocardioides sp. PD653 genes *hcbA1*, *hcbA2*, and *hcbA3* encode enzymes that catalyze the oxidative dehalogenation of hexachlorobenzene (HCB), which is one of the most recalcitrant persistent organic pollutants (POPs). In this study, HcbA1, HcbA2, and HcbA3 were heterologously expressed and characterized. Among the flavin species tested, HcbA3 showed the highest affinity for FMN with a K_d value of $0.75 \pm 0.17\,\mu$M. Kinetic assays revealed that HcbA3 followed a ping-pong bi–bi mechanism for the reduction of flavins. The K_m for NADH and FMN was $51.66 \pm 11.58\,\mu$M and $4.43 \pm 0.69\,\mu$M, respectively. For both NADH and FMN, the V_{max} and k_{cat} were $2.21 \pm 0.86\,\mu$M and $66.74 \pm 5.91\,sec^{-1}$, respectively. We also successfully reconstituted the oxidative dehalogenase reaction *in vitro*, which consisted of HcbA1, HcbA3, FMN, and NADH, suggesting that HcbA3 may be the partner reductase component for HcbA1 in *Nocardioides* sp. PD653.

Keywords: *Nocardioides* sp. PD653, hexachlorobenzene, flavin reductase, TC-FDM, HcbA3.

Electronic supplementary materials: The online version of this article contains supplementary materials (Supplemental Figure S1), which are available at http://www.jstage.jst.go.jp/browse/jpestics/.

Introduction

Hexachlorobenzene (C_6Cl_6; HCB) was first introduced in the 1940s as an organochlorine fungicide for crop seeds[1)] and is one of the most persistent environmental pollutants, whose average half-life in soil is approximately 9 years. Due to its persistence in the environment and tendency to bioaccumulate, it was listed as a persistent organic pollutant at the Stockholm Convention in 2001. *Nocardioides* sp. PD653 (PD653) is a wild-type bacterium capable of mineralizing HCB under aerobic conditions[2)] and has been isolated and studied for the bioremediation of HCB-contaminated sites. PD653 can dehalogenate and hydroxylate HCB in the first step of the HCB mineralization pathway to form pentachlorophenol (C_6HCl_5O; PCP), and the genes *hcbA1*, *hcbA2*, and *hcbA3* have been identified as being involved in catalyzing this reaction.[3)] However, the links between phenotypes and genotypes in PD653 remain unclear due to the lack of gene deletions and complementation systems in *Nocardioides*.

From the deduced amino acid sequences of HcbA1, HcbA2, and HcbA3, we hypothesized that the mechanism was closely related to the two-component flavin-diffusible monooxygenase (TC-FDM) systems, which are comprised of flavin-dependent monooxygenase and its partner reductase component.[4,5)] In these systems, the reductase components generate reduced flavins, which are transferred to oxygenase enzymes for monooxygenation reactions accompanied by the formation of a hydroperoxyflavin or peroxyflavin intermediate. Purified HcbA1 dehalogenates HCB in the presence of an *Escherichia coli* flavin reductase (Fre),[6)] FMN, and NADH, resulting in the formation of flavin-N5-oxide.[7)] These results are consistent with our hypothesis and imply the presence of a partner reductase component of HcbA1. Notably, the co-expression of *hcbA1* and *hcbA3* leads to HCB dehalogenase activity in *E. coli* cells; hence, HcbA3 is believed to supply reduced flavin *in vivo*. However, detailed characterization and identification of HcbA3 functions remain to be achieved. To test our hypothesis noted above, we purified C-terminally His-tagged HcbA1, HcbA2, and HcbA3 and evaluated HcbA3 as an NADH:FMN oxidoreductase. Then the oxidative HCB dechlorination was reconstituted *in vitro* with

* To whom correspondence should be addressed.
E-mail: ktakagi@affrc.go.jp
Published online June 24, 2020

Table 1. Bacterial strain and plasmid used in this study

Strain or plasmid	Relevant characteristics	Reference or origin
Strains		
Nocardioides sp. PD653	HCB^+	2
E. coli DH5α	F^-, l^-, f80d*lac*ZDM15, D(*lac*ZYA-*arg*F)U169, *deo*R, *rec*A1, *end*A1, hsdR17(rk−, mk+), *pho*A, supE44, *thi-1*, *gyr*A96, *rel*A1	TOYOBO
Rhodococcus erythropolis L88	A lysozyme sensitive mutant derived from *Rhodococcus erythropolis* JCM3201	Hokkaido system science Co., Ltd.
Plasmids		
pNitRC1	*E. coli-R. erythropolis* shuttle vector, Ap^r for DH5α, Cm^r for L88, P_{nit}, *rep* (pRE8424)	Hokkaido system science Co., Ltd.
pCpiRC1	*E. coli-R. erythropolis* shuttle vector, Ap^r for DH5α, Cm^r for L88, P_{cpi}, *rep* (pRE8424)	Hokkaido system science Co., Ltd.
pCpiRC1(*hcbA1*)$_{C\text{-}His}$	pCpiRC1 with PCR-amplified DNA fragment of *hcbA1*	This study
pCpiRC1(*hcbA2*)$_{C\text{-}His}$	pCpiRC1 with PCR-amplified DNA fragment of *hcbA2*	This study
pNitRC1(*hcbA3*)$_{C\text{-}His}$	pNitRC1 with PCR-amplified DNA fragment of *hcbA3*	This study

HCB^+, ability of degrade HCB; Ap^r, ampicillin resistant; Cm^r, chloramphenicol resistant.

$HcbA1_{C\text{-}His}$ and $HcbA3_{C\text{-}His}$.

Materials and Methods

1. Bacterial strains and plasmids

The bacterial strains and plasmids used in this study are listed in Table 1. A preculture medium for PD653 was prepared as described previously.[3] *Rhodococcus erythropolis* and *E. coli* strains were routinely cultured in lysogeny broth (LB; 1% Bacto tryptone, 0.5% Bacto yeast extract, and 1% NaCl) with 1.5% agar added for culturing on agar plates. *Escherichia coli* DH5α and *Rhodococcus* transformants were selected using an LB medium containing 100 $\mu g\,mL^{-1}$ ampicillin and 20 $\mu g\,mL^{-1}$ chloramphenicol, respectively.

2. Chemicals

HCB was purchased from Dr. Ehrenstorfer GmbH (Augsburg, Germany). PCP was purchased from Wako Pure Chemical Industries (Osaka, Japan). NADH, nicotinamide adenine dinucleotide phosphate (NADPH), riboflavin, flavin adenine dinucleotide (FAD), and FMN were purchased from TCI Tokyo Kasei (Tokyo, Japan).

3. DNA isolation

Total DNA was purified from PD653 grown on a preculture medium using a DNeasy Tissue Kit (Qiagen, Valencia, CA, USA). Plasmids from recombinant *E. coli* cells were isolated using sodium dodecyl sulfate (SDS) and alkaline lysis as described elsewhere.[36]

4. Construction of plasmids pCpiRC1(hcbA1)$_{C\text{-}His}$, pCpiRC1(hcbA2)$_{C\text{-}His}$, and pNitRC1(hcbA3)$_{C\text{-}His}$

The primers synthesized to amplify *hcbA* genes are listed in Table 2. Genomic DNA from PD653 was used as a template for the PCR experiments described below. The region containing the open reading frame (ORF) of HCB oxidative dehalogenase HcbA1 was amplified using primer set pCRA1_F with pCpiRC1(hcbA1) His_R as a template. A PCR-amplified fragment containing *hcbA1* was subjected to a seamless ligation cloning extract (SLiCE) reaction[8] with NcoI- and XhoI-digested pCpiRC1. The resultant plasmid was designated as pCpiRC1(*hcbA1*)$_{C\text{-}His}$. Plasmid pCpiRC1(*hcbA2*)$_{C\text{-}His}$, which included the ORF of the putative flavin reductase component HcbA2, was constructed in a similar manner using primer set pCRA2_F and pCpiRC1(hcbA2)His_R. Plasmid pNitRC1(*hcbA3*)$_{C\text{-}His}$ was generated by PCR amplifying the fragment containing *hcbA3* using primer set pTRA3_F and pNitRC1(hcbA3)His_R. The PCR-amplified fragment containing ORF3 was subjected to a SLiCE reaction with NcoI- and

Table 2. Specific primers used for amplification of *hcbA* genes

Primer	5′ to 3′
pCRA1_F	GAGATGGAGTCTTGCCATGGTGCGGGATACCCTTGTA
pCpiRC1(hcbA1) His_R	TGGTGATGGTGATGCTCGAAGGAGAAGATGCCCCGAT
pCRA2_F	GAGATGGAGTCTTGCCATGAACCTCGTCACCGTCATC
pCpiRC1(hcbA2)His_R	TGGTGATGGTGATGCTCGAATGAGCGAGTGCTTTCCA
pTRA3_F	AAGAAGGAGATATACCATGACCACCTCCGCACCGATC
pNitRC1(hcbA3)His_R	TGGTGATGGTGATGCTCGAAGGCGGTGGTGAGGCGCT

XhoI- digested pNitRC1. The recombinant plasmids were sequenced for verification. One-hundred nanograms of plasmids was added to 40 μL of *R. erythropolis* L88 electrocompetent cells containing 10% glycerol in a 2 mm gap electroporation cuvette. Cells were transformed using a MicroPulser Electroporator (Bio-Rad, Hercules, CA, USA) with a 2.5 kV pulse (time constant 4.8–5.2), rescued with 1 mL of LB, and incubated for 3 hr at 28°C with shaking at 180 rpm. Cells were plated onto LB agar plates containing chloramphenicol and incubated at 28°C for 5–7 day.

5. Heterologous expression and purification of C-terminally His-tagged proteins

Cells from a single colony of recombinant *R. erythropolis* cells were inoculated into 20 mL of LB and incubated with shaking at 28°C, 180 rpm, for 3–5 day until they reached the stationary phase. The culture was diluted to 1 : 10 in 100 mL of LB, and protein expression was induced with shaking at 28°C, 180 rpm, for 48 hr. The expression of $HcbA3_{C\text{-}His}$ was induced at 20°C to increase the yield of the soluble form of the enzyme. The lysates were cleared and subjected to immobilized metal affinity chromatography (Bio-Rad) at 4°C, and the target proteins were purified according to the manufacturer's instructions. The concentration of imidazole for elution was 100 mM for both $HcbA1_{C\text{-}His}$ and $HcbA3_{C\text{-}His}$ and 200 mM for $HcbA2_{C\text{-}His}$.

6. pH and ionic strength optimization

The optimal pH for $HcbA3_{C\text{-}His}$ activity was determined in a 200 mM acetate buffer (pH 4.6–5.6), 200 mM phosphate buffer (pH 5.7–8.0), 200 mM Tris–HCl buffer (pH 7.2–8.6), and 200 mM glycine-NaOH buffer (pH 8.6–10) at 20°C in total volumes of 1 mL. The enzyme activity at ionic strengths ranging from 10 to 160 mM KP_i (pH 7.5) was also tested using a similar approach.

7. Fluorescence measurement of dissociation constants

The binding of flavins (riboflavin, FAD, and FMN) to $HcbA3_{C\text{-}His}$ was determined by spectrofluorometric titration, monitoring the decreased relative flavin emission intensity due to the fluorescence quenching of flavin upon $HcbA3_{C\text{-}His}$ binding. A 50 nM solution of flavin in 20 mM KP_i buffer, pH 7.5, at 20°C was titrated with increasing concentrations of $HcbA3_{C\text{-}His}$ (0.157–2.814 μM). Spectra were recorded using a BioSpectrometer fluorescence (Eppendorf, Hamburg, Germany) with an excitation wavelength of 470 nm and emission measurements at 520 nm. Emission and excitation bandwidths were set at 25 and 15 nm, respectively. Titrations were performed in triplicate, and K_d values were obtained by determining the amount of bound FMN according to the following equation [Eq. (1)], which was modified from Gao and Ellis[9]:

$$[\text{Enzyme}]_{\text{bound}} = [\text{flavin}]\left[\frac{I_0 - I_C}{I_0 - I_f}\right] \quad (1)$$

where $[\text{Enzyme}]_{\text{bound}}$ represents the concentration of $HcbA3_{C\text{-}His}$ bound to flavin, [flavin] represents the initial concentration of flavin, I_0 is the initial fluorescence intensity of flavin prior to the addition of a substrate, I_C is the fluorescence intensity of the flavin following each substrate addition, and I_f is the final fluorescence intensity. The concentrations of bound $HcbA3_{C\text{-}His}$ were plotted against total $HcbA3_{C\text{-}His}$ concentrations and fitted according to equation Eq. (2) as previously described.[9]

$$y = \frac{(K_d + x + n) - \sqrt{(K_d + x + n)^2 - 4xn}}{2} \quad (2)$$

Briefly, y and x represent the concentration of bound and total $HcbA3_{C\text{-}His}$, respectively, following each substrate addition, and n represents the binding capacity of $HcbA3_{C\text{-}His}$.

8. HcbA1 and HcbA3 enzymatic assays

8.1. Steady-state kinetic measurements of HcbA3 NADH:FMN oxidoreductase activity

Enzymatic assays to measure $HcbA3_{C\text{-}His}$ activity were performed by monitoring the oxidation of NADH to NAD^+ (ε_{340}=6.22 mM^{-1} cm^{-1}) using a V-630Bio UV-Visible spectrophotometer (JASCO, Tokyo, Japan). Reactions were initiated by the addition of $HcbA3_{C\text{-}His}$ (25 nM) to 1 mL reaction mixtures containing 10–120 μM NADH and 1–8 μM FMN in a 20 mM KPi buffer (pH 7.5) at 20°C. Experiments were performed in triplicate. Enzyme activities were determined during the linear portions of the progress curves, with less than 10% of the reduced pyridine nucleotide being utilized over the time course of the reaction. The data from assays were fitted using the Enzfitter software package (Biosoft, Cambridge, UK) according to the ping-pong mechanism [Eq. (3)]:

$$V = \frac{V_{\max}\text{AB}}{K_a\text{B} + K_b\text{A} + \text{AB}} \quad (3)$$

where A and B are the substrate concentrations and K_a and K_b represent the Michaelis constants for substrates A and B, respectively. According to this equation, the actual value of V_{max} and k_{cat} were the same for both substrates (NADH and FMN).

8.2. HcbA1 oxidative dehalogenase activity against HCB

Oxidative dehalogenase assays were performed by measuring the HcbA1 activity at 28°C, 150 rpm, for 60 min. The reaction mixture composition was as follows: 20 mM phosphate buffer (pH 7.5), 240 μM NADH, 50 mM glucose, 0.7 U mL^{-1} glucose dehydrogenase, 555 U mL^{-1} catalase, 8 μM FMN, 17.5 μM HCB, 500 nM $HcbA1_{C\text{-}His}$, and 71.4 nM $HcbA3_{C\text{-}His}$ (at a molar ratio of 7 : 1). The total volume of the reaction mixture was 500 μL. A stock solution of HCB was prepared at 500 mg L^{-1} in methanol, and 5 μL of this solution was added to each of a series of the reaction mixtures in 10 mL glass-stoppered test tube. The reactions were initiated by adding NADH to the reaction mixture, then stopped by adding 1 mL of acetonitrile at 0, 10, 20, 40 and 60 min. After centrifugation at 15,500×g for 10 min, the concentrations of HCB and PCP in the supernatants were quantified using high-performance liquid chromatography (HPLC).

9. Analytical methods

Protein concentrations were determined using the Bradford assay with bovine serum albumin as a standard. Enzyme purity and size were estimated *via* SDS polyacrylamide gel electrophoresis (SDS-PAGE; Bio-Rad) using 12% polyacrylamide gels under denaturing conditions and a Mini-PROTEAN Tetra cell (Bio-Rad). HCB and PCP amounts were determined *via* HPLC using a Hewlett-Packard series 1100 system (Hewlett-Packard, Waldbronn, Germany) with UV absorption measured at 220 nm. Analysis was performed using a ZORBAX Eclipse XDB-C18 column (4.4 mm ×150 mm, 5 μm particle size; Agilent Technologies, Tokyo, Japan). The mobile phase was acetonitrile/0.1% aqueous phosphoric acid (v/v=90/10).

Results

1. Expression and purification of C-terminally histidine-tagged HcbA1 and HcbA3

Recombinant HcbA1, HcbA2, and HcbA3 were overexpressed in *R. erythropolis* L88 and purified (Fig. 1). Each purified protein preparation was colorless and did not exhibit any typical flavin adsorption spectrum of flavin-containing flavoproteins, suggesting that the purified proteins did not contain any bound flavin cofactor.

2. Optimal conditions for enzymatic activity of the purified HcbA3$_{C\text{-}His}$

The effects of temperature, pH, and ionic strength on HcbA3$_{C\text{-}His}$ activity were determined. The optimal pH for HcbA3$_{C\text{-}His}$ flavin reductase activity was between 7.0 and 8.6. At pH 7.0, 7.2, and 8.0, the enzyme activity levels in 100 mM phosphate buffer were approximately 50.2, 88.1, and 81.1%, respectively, relative to that at pH 7.5. HcbA3$_{C\text{-}His}$ showed the highest flavin reductase activity in 60 mM KP$_i$ buffer.

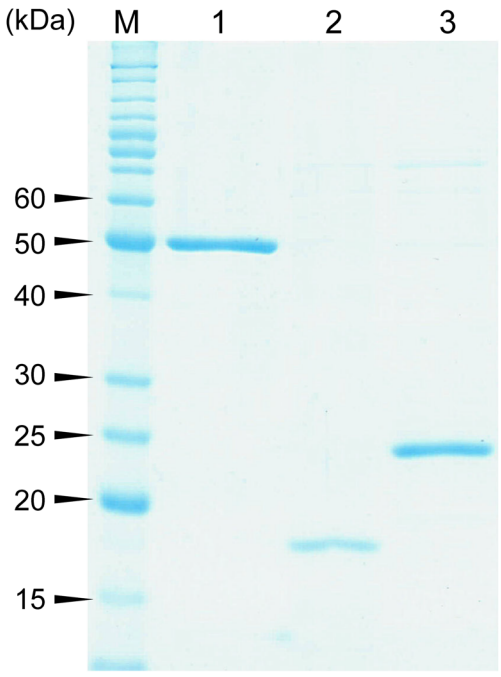

Fig. 1. Purified C-terminally histidine-tagged HcbA1, HcbA2, and HcbA3 as shown by SDS-PAGE. Lane M, marker proteins; lane 1, oxidative HCB dehalogenase HcbA1$_{C\text{-}His}$; lane 2, putative flavin reductase HcbA2$_{C\text{-}His}$; lane 3, NADH:FMN oxidoreductase HcbA3$_{C\text{-}His}$.

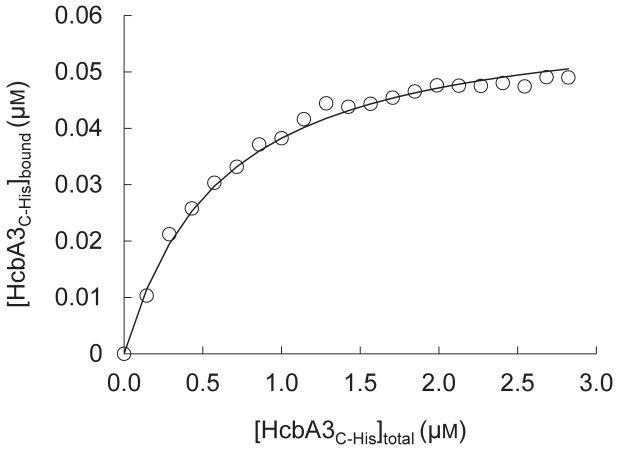

Fig. 2. Fluorometric titration of FMN with the HcbA3$_{C\text{-}His}$ enzyme. Changes in the fluorescence of flavin following the addition of HcbA3$_{C\text{-}His}$ were used to estimate the concentration of bound HcbA3$_{C\text{-}His}$.

3. Flavin-binding studies

Upon the binding of FMN to HcbA3$_{C\text{-}His}$, the fluorescence-emission intensity of FMN decreased, while this was not seen with riboflavin and FAD. This quenching of FMN fluorescence by HcbA3$_{C\text{-}His}$ was used to evaluate the dissociation constant of FMN binding by HcbA3$_{C\text{-}His}$. Fifty-nanomolar FMN was titrated with 0.157–2.814 μM HcbA3$_{C\text{-}His}$, with the quenching of FMN fluorescence being monitored at 520 nm. The concentrations of HcbA3$_{C\text{-}His}$ bound to flavin were plotted against the total HcbA3$_{C\text{-}His}$ concentrations added to each aliquot (Fig. 2). A K_d value of 0.75±0.17 μM for HcbA3$_{C\text{-}His}$ binding to FMN were calculated according to Eq. (2). No fluorescence quenching was observed when flavins were titrated with HcbA1$_{C\text{-}His}$ (0.073–0.16 μM) or HcbA2$_{C\text{-}His}$ (0.014–0.28 μM).

4. Steady-state kinetic analysis of HcbA3$_{C\text{-}His}$

When NADH was used as a pyridinic substrate of HcbA3$_{C\text{-}His}$ in combination with FMN, a distinct activity was detected, while it was not with NADPH. FMN was the preferred flavin substrate of HcbA3$_{C\text{-}His}$ as compared to FAD and riboflavin. Therefore, the steady-state kinetic parameters of HcbA3$_{C\text{-}His}$ were measured in the presence of both FMN and NADH. The initial rates of NADH oxidation followed typical Michaelis–Menten kinetics (Fig. S1), and Lineweaver–Burk plots showed parallel patterns for a ping-pong mechanism (Fig. 3). Therefore, the kinetic parameters could be calculated using Eq. (3) to yield K_m values for NADH and FMN, which were 51.66±11.58 μM and 4.43±0.69 μM, respectively. The V_{max} and k_{cat} values for both substrates were 2.21±0.86 μM and 66.74±5.91 sec^{-1}, respective-

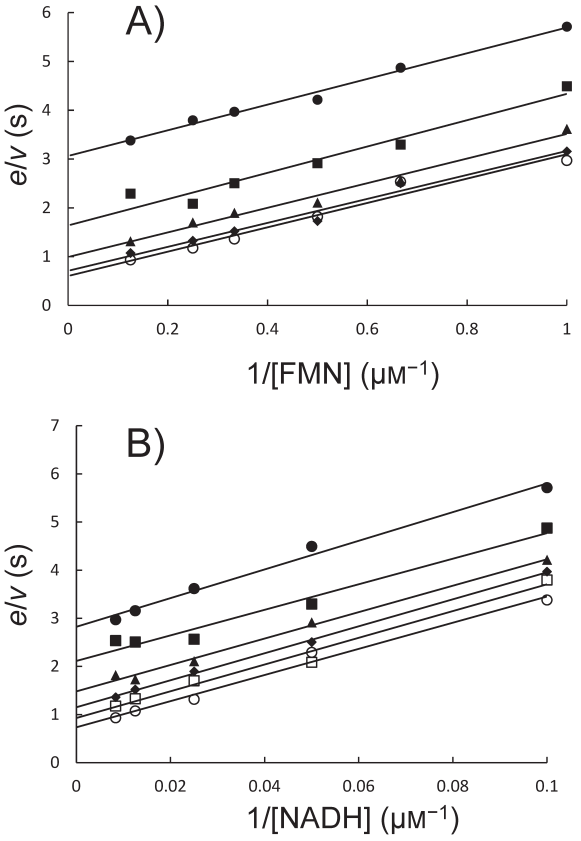

Fig. 3. Double reciprocal plots of $HcbA3_{C\text{-}His}$ steady-state kinetics. (a) Assays were performed using 25 nM $HcbA3_{C\text{-}His}$, 1–8 μM FMN, and various fixed concentrations of NADH, including 10 μM (●), 20 μM (■), 40 μM (▲), 80 μM (◆), and 120 μM (○). (b) Assays were performed using 25 nM $HcbA3_{C\text{-}His}$, 10–120 μM NADH, and various fixed concentrations of FMN, including 1 μM (●), 1.5 μM (■), 2 μM (▲), 3 μM (◆), 4 μM (○), and 8 μM (□).

ly. We concluded that HcbA3 is an NADH:FMN oxidoreductase.

5. Reconstitution of $HcbA3_{C\text{-}His}$ oxidative dehalogenase activity against HCB

Although we demonstrated that $HcbA3_{C\text{-}His}$ generated reduced flavin *in vitro*, it was important to investigate whether this activity led to the dehalogenation of HCB by $HcbA1_{C\text{-}His}$. First, the optimal molar ratio of HcbA1 and HcbA3 was found to be 7:1. The degradation curve of HCB by the enzymes at this ratio is shown in Fig. 4. Briefly, 0.129 μg of HCB was dehalogenated, and 0.124 μg of PCP was generated by 1 μg of $HcbA1_{C\text{-}His}$ in 10 min.

Discussion

Bacteria utilize TC-FDM family enzymes for various reactions, including bioluminescence,[10] oxidation of aromatic compounds,[11] degradation of chelating agents,[12–14] desulfurization of sulfonated compounds,[15–17] and biosynthesis of antibiotics.[18–20] Notably, with respect to the degradation of POPs, single monooxygenase (Ese)[21] has been identified as the enzyme responsible for the metabolism of endosulfan and classified as a TC-FDM. A common feature of all of TC-FDM enzymes is that the flavin reductase supplies reduced flavin for the partner oxygenase component by catalyzing the reduction of oxidized flavin with reducing equivalents provided by a pyridine nucleotide. Furthermore, the genes expressing the reductase and monooxygenase enzymes are often located in the same operon. These features are shared with the oxidative HCB dehalogenase gene *hcbA1* and putative flavin reductase gene *hcbA3*. Purified HcbA1 displays HCB dehalogenase activity with photoreduced FMN and molecular oxygen *in vitro*.[7] However, due to the lack of biochemical analysis of the flavin reductase component, it remained unclear whether the oxidative HCB dehalogenation was catalyzed by a TC-FDM system. Thus, the goal of the current study was to first characterize the flavin reductase component in a single-enzyme assay and then clarify whether HCB dehalogenation was catalyzed in a coupled assay with HcbA1.

Three proteins were expressed by *R. erythropolis* L88 and purified: HcbA1, HcbA2, and HcbA3. Binding analysis revealed that $HcbA3_{C\text{-}His}$ was able to bind to FMN, while $HcbA1_{C\text{-}His}$ and $HcbA2_{C\text{-}His}$ could not. In addition, as shown in the steady-state kinetic analysis, $HcbA3_{C\text{-}His}$ oxidized NADH in the presence of FMN, indicating that this enzyme can be classified as an NADH:FMN oxidoreductase. The fact that HcbA3 demonstrated a significant affinity for FMN was consistent with a major property of the reductase component in TC-FDM systems. In general, the flavin reductase has a greater affinity for oxidized flavin than that for monooxygenase.[9] The distinct specificity of this flavin reductase indicates that FMN may be a major cosubstrate for the HCB oxidative halogenation reaction by HcbA1 and HcbA3 in PD653. Since the deduced amino acid sequence of HcbA2 was similar to the sequence in EmoB, an NADH:FMN oxidoreductase,[22] we previously predicted that HcbA2 would

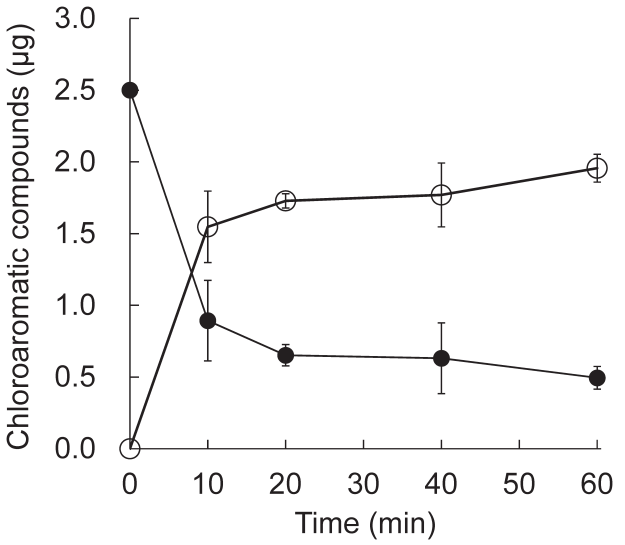

Fig. 4. Conversion of HCB (●) to PCP (○) *via* oxidative dehalogenation of $HcbA1_{C\text{-}His}$–$HcbA3_{C\text{-}His}$. Each error bar indicates the standard error for triplicate samples.

function as a flavin reductase. Nevertheless, $HcbA2_{C\text{-}His}$ did not show any affinity for the flavins tested, nor flavin reductase activity, but only significant inhibition of HCB dehalogenase activity in our coupled assays (data not shown). Hence, the true function of HcbA2 remains unknown.

Based on its secondary structure, flavin reductase HcbA3 is predicted to be similar to TftC,[23] HpaC,[24] PheA2,[25] and CobR.[26] Reactions with TftC and PheA2 proceed according to a sequential and ping-pong bi–bi mechanism, respectively.[25,27] To determine the kinetic mechanism of $HcbA3_{C\text{-}His}$, steady-state kinetic analyses in association with both FMN and NADH were performed. It was determined that HcbA3 reduced flavins *via* a ping-pong bi-bi mechanism. In the TC-FDM family of enzymes, in addition to PheA2, the NADPH-preferring flavin reductase FRP also follows this type of mechanism in single enzyme assays.[28] Both PheA2 and FRP contain flavins as prosthetic groups, which mediate the proton transfer from pyridinic substrates to exogenously added flavin substrates. On the other hand, $HcbA3_{C\text{-}His}$ does not have such flavin cofactors. Thus, it will be hypothesized that a mechanism independent on flavin cofactor is involved in HcbA3 oxidoreductase activity.

We determined that HcbA3 was a possible flavin reductase partner component of HcbA1 in the oxidative HCB dehalogenation system of PD653. Successful dehalogenation of HCB by these two components will allow us to investigate the mechanism involved in reduced flavin transfer. Since reduced flavins generated in HcbA3-catalyzed reactions are unstable due to susceptibility to oxidation by molecular oxygen, they should be rapidly diffused from reductase to monooxygenase. The flavin transfer may occur either through a diffusion mechanism or *via* direct flavin transfer involving protein–protein interactions (PPIs). There are several cases involving PPIs between monooxygenase and a flavin reductase for the transfer of reduced flavin, including FRP–luciferase in *Vibrio harveyi*,[29] SsuE–SsuD in *E. coli*,[30] EmoA–EmoB in *Mesorhizobium* sp. BNC1,[22] and PrnF–PrnD in *Pseudomonas fluorescens* Pf-5.[31] To evaluate the PPIs between HcbA1 and HcbA3, we performed a pull-down assay using a metal affinity column and C-terminally 6×His-tagged proteins. In this assay, each enzyme was independently bound to the column as the bite protein and cell lysates containing other proteins that lacked a fusion tag as a prey protein were loaded onto the columns. These assays, however, provided no conclusive evidence for the presence of specific interactions of these components. Additionally, fluorometric titration of flavin-binding $HcbA3_{C\text{-}His}$ exhibited no fluorescence changes following each addition of $HcbA1_{C\text{-}His}$ (unpublished data). From these findings, it may be speculated that there was no transient interaction between these two components.

In summary, the NADH:FMN oxidoreductase HcbA3 was purified and characterized for the first time in this study. We demonstrated that HCB was dehalogenated to PCP by $HcbA1_{C\text{-}His}$ in concert with $HcbA3_{C\text{-}His}$, suggesting that oxidative HCB dehalogenation may occur through a TC-FDM system in bacteria. We believe these results provide greater insight into how bacteria dehalogenate POPs and identify a potentially novel enzymatic bioremediation technique. Eibes *et al.* summarized works on the bioremediation of organic pollutants in soil using enzymes.[32] Several papers argue that enzymatic bioremediation is suitable for extracellular enzymes that maintain stable activity under operational conditions and have no dependency on expensive coenzymes or cofactors such as NAD(P)H, reduced flavin, and glutathione.[33–35] Given these requirements, the application of HcbA1 to soils is likely to be difficult, but eliminating these bottlenecks should expand the use of bacterial enzymes with diverse metabolic capacities.

Acknowledgements

This work was funded by grant from JSPS KAKENHI (grant number 18H02319).

References

1) J. L. Barber, A. J. Sweetman, D. van Wijk and K. C. Jones: *Sci. Total Environ.* **349**, 1–44 (2005).
2) K. Takagi, A. Iwasaki, I. Kamei, K. Satsuma, Y. Yoshioka and N. Harada: *Appl. Environ. Microbiol.* **75**, 4452–4458 (2009).
3) K. Ito, K. Takagi, A. Iwasaki, N. Tanaka, Y. Kanesaki, F. Martin-Laurent and S. Igimi: *Appl. Environ. Microbiol.* **83**, e00824–e17 (2017).
4) H. R. Ellis: *Arch. Biochem. Biophys.* **497**, 1–12 (2010).
5) M. M. E. Huijbers, S. Montersino, A. H. Westphal, D. Tischler and W. J. H. van Berkel: *Arch. Biochem. Biophys.* **544**, 2–17 (2014).
6) L. Xun and E. R. Sandvik: *Appl. Environ. Microbiol.* **66**, 481–486 (2000).
7) S. Adak and T. P. Begley: *Biochemistry* **58**, 1181–1183 (2019).
8) Y. Okegawa and K. Motohashi: *Biochem. Biophys. Rep.* **4**, 148–151 (2015).
9) B. Gao and H. R. Ellis: *Biochem. Biophys. Res. Commun.* **331**, 1137–1145 (2005).
10) E. A. Meighen: *Microbiol. Rev.* **55**, 123–142 (1991).
11) U. Arunachalam, V. Massey and C. S. Vaidyanathan: *J. Biol. Chem.* **267**, 25848–25855 (1992).
12) T. Uetz, R. Schneider, M. Snozzi and T. Egli: *J. Bacteriol.* **174**, 1179–1188 (1992).
13) H. R. Knobel, T. Egli and J. R. van der Meer: *J. Bacteriol.* **178**, 6123–6132 (1996).
14) Y. Xu, M. W. Mortimer, T. S. Fisher, M. L. Kahn, F. J. Brockman and L. Xun: *J. Bacteriol.* **179**, 1112–1116 (1997).
15) K. A. Gray, G. T. Mrachko and C. H. Squires: *Curr. Opin. Microbiol.* **6**, 229–235 (2003).
16) J. R. van der Ploeg, R. Iwanicka-Nowicka, T. Bykowski, M. M. Hryniewicz and T. Leisinger: *J. Biol. Chem.* **274**, 29358–29365 (1999).
17) E. Eichhorn, J. R. van der Ploeg and T. Leisinger: *J. Biol. Chem.* **274**, 26639–26646 (1999).
18) S. G. Kendrew, S. E. Harding, D. A. Hopwood and E. N. Marsh: *J. Biol. Chem.* **270**, 17339–17343 (1995).
19) L. Filisetti, M. Fontecave and V. Niviére: *J. Biol. Chem.* **278**, 296–303 (2003).
20) J. Valton, C. Mathevon, M. Fontecave, V. Niviére and D. P. Ballou: *J. Biol. Chem.* **283**, 10287–10296 (2008).
21) K. M. Weir, T. D. Sutherland, I. Horne, R. J. Russell and J. G. Oakeshott: *Appl. Environ. Microbiol.* **72**, 3524–3530 (2006).
22) J. Bohuslavek, J. W. Payne, Y. Liu, H. J. Bolton Jr. and L. Xun: *Appl.*

Environ. Microbiol. **67**, 688–695 (2001).
23) M. R. Gisi and L. Xun: *J. Bacteriol.* **185**, 2786–2792 (2003).
24) B. Galán, E. Díaz, M. A. Prieto and J. L. García: *J. Bacteriol.* **182**, 627–636 (2000).
25) U. Kirchner, A. H. Westphal, R. Müller and J. H. van Berkel: *J. Biol. Chem.* **279**, 47545–47553 (2003).
26) A. D. Lawrence, S. L. Taylor, A. Scott, M. L. Rowe, C. M. Johnson, S. E. J. Rigby, M. A. Geeves, R. W. Pickersgill, M. J. Howard and M. J. Warren: *Biosci. Rep.* **34**, e00120 (2014).
27) B. N. Webb, J. W. Ballinger, E. Kim, S. M. Belchik, K. S. Lam, B. Youn, M. S. Nissen, L. Xun and C. Kang: *J. Biol. Chem.* **285**, 2014–2027 (2010).
28) B. Lei and S. C. Tu: *Biochemistry* **37**, 14623–14629 (1998).
29) J. C. Low and S. C. Tu: *Photochem. Photobiol.* **77**, 446–452 (2003).
30) K. Abdurachim and H. R. Ellis: *J. Bacteriol.* **188**, 8153–8159 (2006).
31) J. K. Lee and H. Zhao: *J. Bacteriol.* **189**, 8556–8563 (2007).
32) G. Eibes, A. Arca-Ramos, G. Feijoo, J. M. Lema and M. T. Moreira: *Appl. Microbiol. Biotechnol.* **99**, 8815–8829 (2015).
33) C. Scott, G. Pandey, C. Hartley, C. Jackson, M. Cheesman, M. Taylor, R. Pandey, J. Khurana, M. Teese, C. Coppin, K. Weir, R. Jain, R. Lal, R. Russell and J. Oakeshott: *Indian J. Microbiol.* **48**, 65–79 (2008).
34) T. D. Sutherland, I. Horne, K. M. Weir, C. W. Coppin, M. R. Williams, M. Selleck, R. J. Russell and J. G. Oakshott: *Clin. Exp. Pharmacol. Physiol.* **31**, 817–821 (2004).
35) R. J. Russell, R. L. Harcourt and J. G. Oakshott: *ACIAR Proc.* **85**, 341-348 (1998).
36) H. C. Birnboim and J. Doly: *Nucleic Acids Res.* **7**, 1513–1523 (1979).